

MIMO Radar Aided mmWave Time-Varying Channel Estimation in MU-MIMO V2X Communications

Sai Huang¹, Member, IEEE, Meng Zhang², Graduate Student Member, IEEE,
Yicheng Gao¹, Student Member, IEEE, and Zhiyong Feng¹, Senior Member, IEEE

Abstract—Robust channel estimation in time-varying channels is used to guarantee the quality of communication services, especially for Vehicle-to-Everything (V2X) scenarios. To improve the channel estimation accuracy and reduce the pilot overhead, multi-input multi-output (MIMO) radar is deployed to assist millimeter wave (mmWave) channel estimation. In this paper, we propose a MIMO radar aided channel estimation scheme using deep learning (DL) for the uplink mmWave multiuser (MU)-MIMO communications. To allocate pilot resources reasonably, we design a transmission frame structure of joint radar module and communication module, which divides the estimation scheme into two stages, i.e., the arrival/departure (AoA/AoDs) estimation stage and the gain estimation stage. In view of the imperfections of array elements in practice, we propose an AoA/AoDs estimation algorithm based on subspace reconstruction in the AoA/AoDs estimation stage named two-step angle estimation (TSAE) algorithm. In the gain estimation stage, a DL based channel gain estimator is designed. An autoencoder combined with residual structure named residual denoising autoencoder (RDAE) is proposed to eliminate the noise on wireless signals, which is passed into the least square (LS) estimation module to obtain gains. Simulation results demonstrate that the MIMO radar aided and DL-based channel estimator provides the efficient estimation performance of the high-mobility mmWave channel with fewer training resources.

Index Terms—Deep learning (DL), millimeter wave (mmWave) communications, multiuser multi-input multi-output (MU-MIMO), MIMO radar, vehicle-to-everything (V2X).

Manuscript received January 20, 2021; revised May 9, 2021; accepted May 22, 2021. Date of publication June 9, 2021; date of current version November 11, 2021. This work was supported in part by the National Natural Science Foundation of China under Grant 61941102, in part by the National Key Research and Development Program of China under Grant 2020YFB1807602 and Grant 2019YFB1804404, in part by the Beijing Natural Science Foundation under Grant 19L2022 and Grant 4202046, in part by the Industrial Internet Innovation and Development Project of Ministry of Industry and Information Technology under Grant TC200H031, and in part by the Key Laboratory of Universal Wireless Communications (Beijing University of Posts and Telecommunications), Ministry of Education, China, under Grant KFKT-2020105. The associate editor coordinating the review of this article and approving it for publication was Y. Gao. (Corresponding author: Zhiyong Feng.)

Sai Huang is with the Key Laboratory of Universal Wireless Communications, Ministry of Education, Wireless Technology Innovation Institute (WTI), Beijing University of Posts and Telecommunications, Beijing 100876, China.

Meng Zhang is with the School of Information and Communication Engineering, Beijing University of Posts and Telecommunications, Beijing 100876, China.

Yicheng Gao is with the Department of Computing, Imperial College London, London SW7 2AZ, U.K.

Zhiyong Feng is with the Key Laboratory of Universal Wireless Communications, Beijing University of Posts and Telecommunications, Beijing 100876, China (e-mail: fengzy@bupt.edu.cn).

Color versions of one or more figures in this article are available at <https://doi.org/10.1109/TWC.2021.3085823>.

Digital Object Identifier 10.1109/TWC.2021.3085823

I. INTRODUCTION

WITH the advent of 5G information era, intelligent terminal devices are showing explosive growth. Applications such as intelligent traffic system (ITS), virtual reality (VR) and ultra-High Definition (HD) video emerge in an endless stream. The increasing demand for various multimedia services leads to a substantial increase in the capacity of the global mobile system, while the scarcity of spectrum resources becomes increasingly apparent [1]. Especially, Vehicle-to-Everything (V2X), as a crucial part of ITS, will face the challenge of user random mobility, i.e., the time-varying channel. The performance of channel estimation technique in physical layer is the premise of the reliable data transmission. Multiple potential technologies have been proposed to meet the challenges in 5G communication scenarios such as the higher data rates and larger bandwidth requirements [2], [3], where millimeter wave (mmWave) and massive multiple-input multiple-output (MIMO) are considered to be promising technologies.

Recently, mmWave communication [4]–[6] has become one of the critical technologies in 5G cellular systems deployment with its ultra-wide (30-300GHz) spectrum resources, which provides Gbps data rates and improves the spectrum efficiency. However, due to its high attenuation and weak penetration, massive MIMO [7]–[9] is required to achieve high-gain directional beamforming. Larger antenna gain through beamforming can be obtained to alleviate the propagation loss and realize sufficient link margin. Beam width decreases with the number of antennas and then the interference among users reduces. Therefore, beamforming is the key to the combination of mmWave and massive MIMO.

Currently, MIMO system is mainly equipped with analog precoder [10], digital precoder [11] and hybrid precoder [12]. Analog precoding only supports single-channel transmission of a single user. Digital precoding can realize multiple channel transmission for multiple users under the premise of high hardware complexity. Hybrid precoding which combines the digital precoders with small number of radio frequency (RF) chains and analog precoders with multiple analog phase shifters (APs), striking the tradeoff between hardware consumption and system performance requirements, is proposed as a compromised solution in the mmWave system.

The prerequisite of optimal beamforming is to obtain complete channel state information (CSI), thus mmWave channel estimation is necessary, especially for the massive MIMO system. CSI estimation methods for mmWave

communications include least squares method (LS), linear minimum mean square error (LMMSE), compressed sensing (CS) and the emerging deep learning (DL) based channel estimation methods. The advantage of LS lies in its low complexity, while it has large estimation error. LMMSE performs high estimation accuracy, but it requires channel statistics and noise variance as prior information, which limits its applications in practice. Under the sparse assumption of angle domain in the mmWave band, plentiful CS-based methods have been proposed [12]–[15]. To alleviate the grid mismatch phenomenon of the quantized angle grids in CS-based methods, an ultra-high resolution estimation algorithm with high complexity is proposed in [12]. The adaptive CS scheme proposed in [15] utilizes hierarchical codebooks and approaches the favorable coverage probability, but only for the channel estimation in single-user scenario. A non-orthogonal pilot design scheme is proposed for frequency division duplex (FDD) system, and a distributed sparse adaptive matching pursuit algorithm (SAMP) is presented in [14] to jointly estimate the multiple subcarriers. However, the schemes in [14], [15] need feedback, which increases the training overhead and estimation latency.

With the rapid development of high mobility communication fields such as unmanned aerial vehicles (UAVs) [16] and high-speed trains (HSTs) [17], the demand for channel estimation algorithms under mobile conditions is gradually increasing. Q. Qin *et al.* in [18] propose a novel transmission frame structure, which divides the estimation of the time-varying channel into two stages. The angles are estimated by an adaptive algorithm as a block-sparse recovery problem, while the quantization error exists due to CS and the training overhead is also large. DL has received widespread attention due to its feature self-learning ability and the enhancement of hardware computing power. On this base, DL has penetrated into wireless communications [19], such as channel coding and decoding [20], channel information feedback [21], beam search [22], beamforming [23], modulation recognition [24], channel estimation, and etc [25]–[27]. Aiming at the highly dynamic vehicle scene, deep neural network (DNN) is used for k -step channel prediction of space-time block codes, and then a decision-oriented channel estimation algorithm is proposed to eliminate the need for channel Doppler frequency shift estimation in [25]. X. Wang *et al.* in [26] proposes two different channel estimation schemes, one is a data-driven end-to-end channel estimator, and the other is a model-driven channel estimator combined with communication knowledge and a small amount of training parameters. In view of the characteristics of rayleigh fading channels, an estimator named SBGRU is proposed in [27], combining RNN structure with sliding window. However, the large amount of training data required for the two schemes leads to the additional training cost. Notably, only the channel matrix without both the estimation of AoA/AoDs and channel gains is obtained according to the mmWave channel model in [27].

Moreover, signal optimization by denoising is also an effective way to improve the estimation accuracy. An end-to-end Super-resolution convolution neural network (SRCNN) [28] is proposed to learn the map between LR/HR images and optimize all layers. Residual learning is widely adopted in the

field of image classification and recognition. Different from the general CNN, the residual network only needs to learn the difference between input and output directly through 'shortcut' structure, which keeps the integrity of input information and reduces the difficulty of model learning. In addition, it alleviates the gradient disappearance caused by the increase of CNN depth. For image restoration, a feed forward denoising convolution neural network (CNN) called DnCNN is designed in [29], where residual learning and batch normalization is utilized to improve the denoising performance. With the evolution of CNN, residual learning also shows similar performance in text and speech processing.

MIMO radar [30] detects and locates targets in all-weather, all-day and long distance. Compared with the traditional phased array radar (PAR), MIMO radar obtains information through parallel multi-channels in space and achieves parameter estimation for multiple targets. Due to the mobility of the receiver, the state of the channel continuously changes in the time domain. In this case, MIMO radar's rapid detection characteristics can play to its advantage, which takes up less overhead. The antenna aperture and spatial diversity gain increases by diversity processing, thus the parameter estimation accuracy improves. For MIMO radar, various direction of arrival (DoA) estimation methods exist such as Capon, MUSIC, ESPRIT, sparse Bayesian learning and etc. [31]–[35]. Array models in aforementioned works are under the assumption that the array elements are accurately calibrated. However, various array imperfections, such as mutual coupling [36], gain and phase errors [37] and location errors [38] exist in practice, resulting the degradation in estimation performance [39]. Works have focused on eliminating or mitigating the estimation error caused by the sensor uncertainties [40]–[44].

Inspired by the above channel estimation algorithms, we propose a MIMO radar aided channel estimation scheme based on DL for the uplink mmWave MU-MIMO communications for a time-varying channel. We focus on multiuser V2X scenarios and only a small number of pilots is utilized to achieve higher estimation accuracy while minimizing training difficulty. The estimation scheme is divided into two parts: angle estimation and gain estimation, in which the latter works with the prior information of the former. The main contributions of the paper can be summarized as follows:

- We design a novel frame structure for the uplink transmission that takes both radar and communication modules into consideration. In each transmission frame, we use the MIMO radar deployed on the road side unit (RSU) to measure the azimuth information of moving vehicles in the first stage. In the second stage, a DL-based complex gain estimator is designed to obtain the channel gain information based on prior angle information.
- MIMO radar is applied to AoA/AoDs estimation in the considered high-mobility communication scenarios. Considering the uncertain deviation of sensors, including several types of error, we propose an AoA/AoDs estimation algorithm based on subspace reconstruction, which is robust to the quantization error. The target UEs' number is derived from the signal covariance matrix and angles are obtained from the new covariance matrix after subspace reconstruction. This stage involves no angle

TABLE I
 THE NOTATIONS OF THIS PAPER

$j \triangleq \sqrt{-1}$	The imaginary unit
$\mathbf{A}^*, \mathbf{A}^T$ and \mathbf{A}^H	Matrix conjugate, transpose and Hermitian transpose
\mathbf{A}^{-1}	Matrix inverse
$[\mathbf{A}]_{i,j}$	Matrix element at the i -th row and j -th column
$\mathbf{A}, \hat{\mathbf{A}}$ and $\tilde{\mathbf{A}}$	Actual, estimated matrix and matrix under array uncertainties
\mathbf{I}_N	$N \times N$ Identity matrix
$ \cdot $	Absolute value
$\ \cdot\ _2, \ \cdot\ _F$	ℓ_2 norms and Frobenius norms
\otimes	Kronecker product
\odot	Khatri-Rao product
$\text{vec}(\mathbf{A})$	Vectorization of \mathbf{A}
$\text{diag}(\mathbf{a})$	Diagonal matrix with \mathbf{a}
$\mathcal{N}(\mu, \sigma)$	Gaussian distribution with mean μ and covariance σ
$\mathcal{CN}(\mu, \sigma)$	Complex Gaussian distribution with mean μ and covariance σ
$E[\cdot]$	Expected value
$\text{tr}\{\mathbf{A}\}$	The trace of the matrix \mathbf{A}

quantization. Benefit from the powerful detection performance of MIMO radar, the algorithm achieves higher estimation accuracy.

- We design a supervised DL-based channel gain estimator, which is composed of a denoising autoencoder (DAE) and LS estimator. The DAE introduces a residual structure and Gaussian noise layers to filter part of the complex noise with a smaller amount of data and iterations, which improves the anti-noise and anti-movement robustness. Under the condition of a limited number of pilots, beamforming is implemented obeying the principle of maximizing the pilot signal to noise ratio. Finally, results of the channel gain estimation are obtained.
- We derive the Cramer-Rao Lower bound (CRLB) of the estimation performance and analyze the algorithm complexity of the channel estimation scheme under a single path for each UE. Finally, the performance of the proposed estimation algorithm is evaluated through simulations.

The rest of the paper is organized as follows. In Section II, we present the system model and main assumptions used in the paper. In Section III, we formulate the channel estimation problem and present the idea of the proposed two-stage training scheme. The proposed AoA/AoDs algorithm and path gains estimation algorithm are presented and discussed in Section IV. The performance of proposed algorithms are analyzed in Section V. In Section VI, simulation results demonstrating the performance of the proposed algorithms are given. Section VII concludes the paper.

Notations: A summary of the notation used throughout this manuscript can be found in Table I.

II. SYSTEM MODEL

In this section, we consider a MIMO radar aided multiuser mmWave massive MIMO communication system, as shown in Fig. 1. The MIMO radar is deployed at RSU to assist in

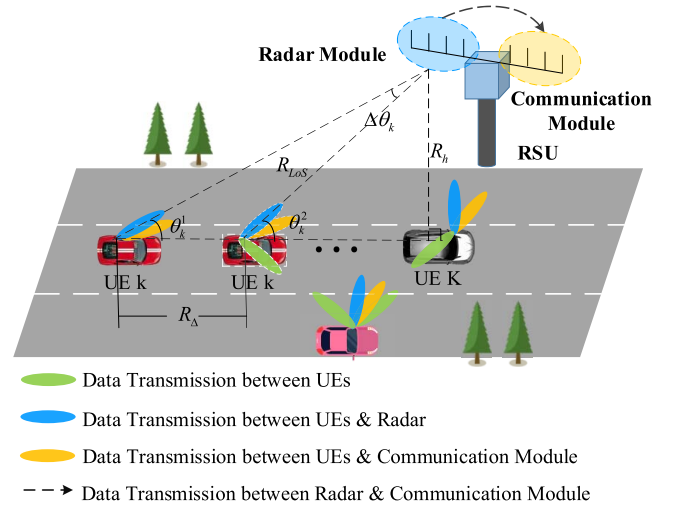


Fig. 1. Radar aided multiuser V2X communication scenario in mmWave system.

channel estimation in V2X scenarios, where the user equipments (UE) in the system are high-speed moving vehicles. It is assumed that the far-field condition is satisfied between the target UEs and the radar. The RSU is equipped with the uniform linear array (ULA) of N antennas to simultaneously serve K UEs, where the antenna array is split into two modules: one for MIMO radar and one for the uplink communications.

Specially, we first introduce the signal model for communication and radar modules respectively with hybrid precoding architectures [45] as shown in Fig. 2. There are the RSU with the wireless communication module and the MIMO radar module on the left and the K vehicles are on the right. Then the mmWave channel model is presented to further formulate a mmWave time-varying channel estimation problem.

A. Signal Model for the Uplink Communications

For the uplink communication module, we consider the RSU with N_{BS} antennas and N_{RF} chains communicates with K UEs simultaneously, where each UE is equipped with N_{UE} antennas and N_u RF chains [11], as shown in Fig. 2. The RSU receives a total of N_s streams sent by each UE, such that $N_s = K$. Without loss of generality, we assume that $N_s \leq N_{RF} \leq N_{BS}$ and $1 \leq N_u \leq N_{UE}$.

The hybrid precoder for the k -th UE at the n -th time slot is denoted by $\mathbf{F}_{n,k} = \mathbf{F}_{RF,k}^{(n)} \mathbf{F}_{BB,k}^{(n)} \in C^{N_{UE} \times N_u}$, where $\mathbf{F}_{BB,k}^{(n)} \in C^{N_u \times N_u}$ is the baseband precoder and $\mathbf{F}_{RF,k}^{(n)} \in C^{N_{UE} \times N_u}$ is the RF precoder. Hence, the transmitted signal vector from the k -th UE can be written as

$$\mathbf{x}_k[n] = \mathbf{F}_{RF,k}^{(n)} \mathbf{F}_{BB,k}^{(n)} \mathbf{s}_k[n] \quad (1)$$

where $\mathbf{s}_k[n] \in C^{N_u \times 1}$ is the transmitted training sequence.

We further apply a hybrid combiner at the RSU side as $\mathbf{W}_{n,k} = \mathbf{W}_{RF,k}^{(n)} \mathbf{W}_{BB,k}^{(n)} \in C^{N_{BS} \times N_s}$, where $\mathbf{W}_{RF,k}^{(n)} \in C^{N_{BS} \times N_{RF}}$ and $\mathbf{W}_{BB,k}^{(n)} \in C^{N_{RF} \times N_s}$ denote the RF combiner and baseband combiner respectively. The received signal can

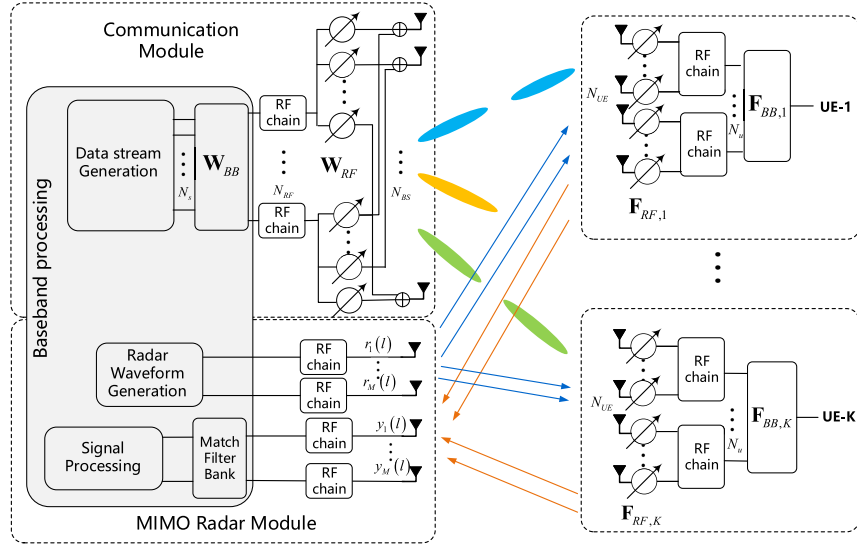


Fig. 2. MIMO radar aided hybrid precoding architectures for multiuser mmWave system.

be given by

$$\mathbf{y}_c^k[n] = \mathbf{W}_{n,k}^H \mathbf{H}_k[n] \sum_{k=1}^K \mathbf{F}_{RF,k}^{(n)} \mathbf{F}_{BB,k}^{(n)} \mathbf{s}_k[n] + \mathbf{W}_{n,k}^H \mathbf{n}_k[n] \quad (2)$$

where $\mathbf{H}_k[n] \in C^{N_{BS} \times N_{UE}}$ is the mmWave channel from the k -th UE to the RSU and $\mathbf{n}_k[n]$ is the Gaussian noise vector obeying $\mathcal{CN}(\mathbf{0}_{N_{BS} \times 1}, \sigma_n^2 \mathbf{I}_{N_{BS}})$.

B. Signal Model for the MIMO Radar

For the MIMO radar module, we consider a monostatic radar application containing N_T and N_R array elements for transmitting and receiving respectively, where $N_T = N_R = M$. The matrix form of transmitted signals for entire N_T elements is presented as

$$\mathbf{r}(l) = [r_1(l), r_2(l), \dots, r_M(l)]^T, \quad l = 1, 2, \dots, L \quad (3)$$

where L is the length of transmitted waveforms, i.e., snapshots. Thus, we acquire the correlation matrix of $\mathbf{r}(l)$ as

$$\mathbf{R}_r = \frac{1}{L} \sum_{l=1}^L \mathbf{r}(l) \mathbf{r}^H(l) \quad (4)$$

We assume the transmitted signals are mutually orthogonal such that the correlation coefficient of different signals equals to zero. The correlation matrix can be reduced to a unit matrix as \mathbf{I}_M , which means the energy is evenly dispersed throughout the spatial domain.

For K target UEs, the corresponding echo signal received by N_R antennas is obtained as

$$\mathbf{y}_r(l) = \sum_{k=1}^K \beta_k \mathbf{b}_r(\theta_k) \mathbf{b}_t^*(\theta_k) \mathbf{r}(l) + \boldsymbol{\omega}(l), \quad l = 1, 2, \dots, L \quad (5)$$

where $\mathbf{y}_r(l) = [y_1(l), y_2(l), \dots, y_{N_R}(l)]^T$, $y_n(l)$ is the echo signal received by the n -th receiving element, $\beta_k \sim \mathcal{CN}(0, \sigma_{\beta_k}^2)$ denotes the reflection coefficient of the k -th UE and $\boldsymbol{\omega}(l) \sim \mathcal{CN}(0, \sigma_{\omega}^2 \mathbf{I}_M)$ represents the noise. Moreover,

$\mathbf{b}_r(\theta_k)$ and $\mathbf{b}_t(\theta_k)$ are the steering vectors for the transmitting and receiving antennas respectively, satisfying

$$\mathbf{b}_t(\theta_k) = [e^{j2\pi f_0 \tau_1(\theta_k)}, e^{j2\pi f_0 \tau_2(\theta_k)}, \dots, e^{j2\pi f_0 \tau_{N_T}(\theta_k)}]^T \quad (6a)$$

$$\mathbf{b}_r(\theta_k) = [e^{j2\pi f_0 \tilde{\tau}_1(\theta_k)}, e^{j2\pi f_0 \tilde{\tau}_2(\theta_k)}, \dots, e^{j2\pi f_0 \tilde{\tau}_{N_T}(\theta_k)}]^T \quad (6b)$$

where f_0 is the carrier frequency of radar signals, $\tau_m(\theta_k)$ and $\tilde{\tau}_m(\theta_k)$ indicate the time to reach and return from the target respectively and θ_k denotes the azimuth angle of the k -th UE.

C. Channel Model

In view of the Doppler effect in V2X communications, we adopt a time-varying geometric channel model consisting of N_L paths. The mmWave channel model $\mathbf{H}_k[n]$ can be expressed as

$$\mathbf{H}_k[n] = \frac{1}{\sqrt{N_L}} \sum_{n_l=1}^{N_L} \alpha_{k,n_l} e^{j2\pi f_d n T_s} \mathbf{a}_{BS}(\phi_{k,n_l}^r) \mathbf{a}_{UE}^H(\phi_{k,n_l}^t) \quad (7)$$

where α_{k,n_l} is the complex channel gain, which obeys Rayleigh distribution, f_d is the Doppler frequency, T_s represents the system sampling period, $\phi_{k,n_l}^r \in [0, \pi]$ and $\phi_{k,n_l}^t \in [0, \pi]$ denote the angle of arrival (AoA) and angle of departure (AoD), respectively. Furthermore, $\mathbf{a}_{BS}(\phi_{k,n_l}^r)$ and $\mathbf{a}_{UE}^H(\phi_{k,n_l}^t)$ are the steering vector at the RSU and UE in the form of ULA, which are given as

$$\mathbf{a}_{BS}(\phi_{k,n_l}^r) = \frac{1}{\sqrt{N_{BS}}} [1, e^{j\xi_r}, \dots, e^{j(N_{BS}-1)\xi_r}]^T \quad (8a)$$

$$\mathbf{a}_{UE}(\phi_{k,n_l}^t) = \frac{1}{\sqrt{N_{UE}}} [1, e^{j\xi_t}, \dots, e^{j(N_{UE}-1)\xi_t}]^T \quad (8b)$$

where $\xi_r = \frac{2\pi}{\lambda_{mW}} d \cos(\phi_{k,n_l}^r)$, $\xi_t = \frac{2\pi}{\lambda_{mW}} d \cos(\phi_{k,n_l}^t)$, λ_{mW} is the wavelength and d is the inter-element spacing, generally set as $\lambda_{mW}/2$. Then the carrier frequency of the

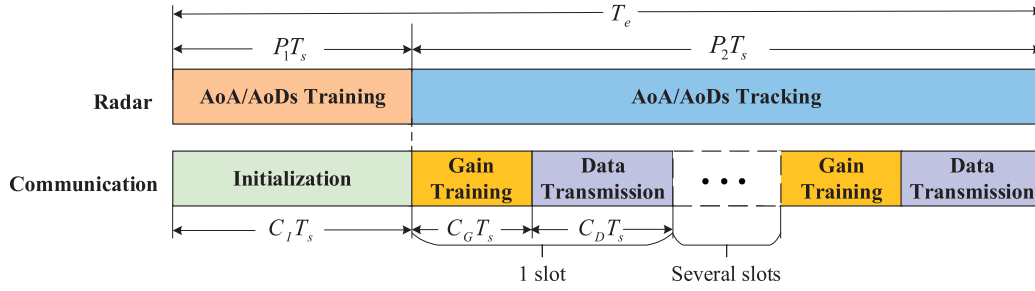


Fig. 3. The structure of uplink transmission frame.

uplink mmWave communications f_{mW} is $f_{mW} = c/\lambda_{mW}$, where c is the speed of the light.

We then rewrite the mmWave channel model in (7) in a matrix form as

$$\mathbf{H}_k[n] = \mathbf{\Lambda}_{BS,k} \text{diag}(\mathbf{A}_{n,k}) \mathbf{\Lambda}_{UE,k}^H \quad (9)$$

where $\mathbf{\Lambda}_{BS,k} \in \mathbb{C}^{N_{BS} \times N_L}$, $\mathbf{\Lambda}_{UE,k}^H \in \mathbb{C}^{N_{UE} \times N_L}$ and $\mathbf{A}_{n,k} \in \mathbb{C}^{N_L \times 1}$ merges the path gain and Doppler effect, satisfying

$$\mathbf{\Lambda}_{BS,k} = [\mathbf{a}_{BS}(\phi_{k,1}^r), \mathbf{a}_{BS}(\phi_{k,2}^r), \dots, \mathbf{a}_{BS}(\phi_{k,N_L}^r)] \quad (10a)$$

$$\mathbf{\Lambda}_{UE,k} = [\mathbf{a}_{BS}(\phi_{k,1}^t), \mathbf{a}_{BS}(\phi_{k,2}^t), \dots, \mathbf{a}_{BS}(\phi_{k,N_L}^t)] \quad (10b)$$

$$\mathbf{A}_{n,k} = [\mathbf{A}_{n,k}^1, \mathbf{A}_{n,k}^2, \dots, \mathbf{A}_{n,k}^{N_L}]^T \quad (10c)$$

III. PROBLEM FORMULATION

In this section, we design a novel frame structure of uplink transmission for MIMO radar aided communication system, which consists of two stages, as shown in Fig. 3. The duration of each frame is T_e , which includes multiple pilots. For the first stage, the transmission frame of the radar module consists of two parts, i.e., AoA/AoDs training and AoA/AoDs tracking denoted by $P_1 T_s$ and $P_2 T_s$, respectively. AoA/AoDs Training corresponds to the total time consumption of AoA/AoDs estimation algorithm with MIMO radar. T_s is the duration of a single pilot and P_1 , P_2 are the number of pilots used by the MIMO radar for angle training and tracking, respectively. For the communication module, initialization is performed in the first C_I pilots, followed by several time slots in the second stage. Assume that $P_1 = C_I$ equals to the number of snapshots. Moreover, each time slot is composed of path gains training and data transmission, corresponding to C_G and C_D pilots respectively. We perform the channel gains estimation during the Gain Training. Note that AoA/AoDs Tracking and Gain Tracking are conducted to predict the current and subsequent channel parameters based on the previous sequence.

In the highly dynamic V2X scenarios, the channel coefficients mainly vary in the UEs' angles and the channel gains according to Equ. (2). The angles are subject to the large-scale characteristics of the scattering environment and the corresponding change is relatively slow, which can be regarded as constant within a certain period of time. The

channel gains are affected by factors such as Doppler frequency offset and their changes are relatively rapid. Therefore, the time-varying channel estimation problem can be divided into a static angle estimation problem and a time-varying gain estimation problem. The relevant proofs and rationality of using MIMO radar are given in Appendix A.

In the V2X scenarios, the antenna of the RSU is generally taller than the moving vehicles. It is obvious that the transmission path between the UEs and RSU are mostly the line-of-sight (LoS). This is suitable for the narrow beams' less scattering and sparseness millimeter wave communications. During the communication occurs between the moving vehicles and the RSU, the radar quickly detects the direction of the targets and then informs RSU separated. Furthermore, due to the sparsity of the mmWave channel, all the paths can be regarded as separate and only one path will be the main beam. In addition, the path gain of the LoS is generally higher than the none-line-of-sight (NLoS) in the outdoor environment [46]. Therefore, we assume the LoS path as the main lobe direction, while other NLoS paths falling into the side lobe directions can be treated as noise and are neglected. In this paper, we assume that RSU transmits signals along the AoAs obtained from the MIMO radar. Hence AoDs and AoAs are equal in value within a transmission frame.

A. AoA/AoDs Estimation With MIMO Radar

As shown in Fig. 4, the workflow of the entire estimation scheme is performed in two main phases: AoA/AoDs estimation phase at the radar module and path gains estimation phase at the communication module, each of which also includes its own sub-phases. Firstly, the latest angle information data is obtained after the radar echo signals are received and processed by the radar module and is the input of the mmWave MIMO system as auxiliary information for the subsequent path gain estimation. Buffers in the mmWave MIMO system hold a large number of previous transmitted signals and are continuously stored in real-time communication signals. In the AoA/AoDs estimation phase, some assumptions are made and three specific types of errors are considered.

We rewrite Equ. (5) as

$$\mathbf{Y}_r = \mathbf{B}_R \text{diag}(\beta_1, \beta_2, \dots, \beta_K) \mathbf{B}_T^H \mathbf{R} + \mathbf{W} \quad (11)$$

where $\mathbf{Y}_r = [\mathbf{y}_r(1), \mathbf{y}_r(2), \dots, \mathbf{y}_r(L)] \in \mathbb{C}^{M \times L}$ and $\mathbf{W} = [\omega(1), \omega(2), \dots, \omega(L)] \in \mathbb{C}^{M \times L}$ indicate the echo signal matrix and noise matrix. $\mathbf{B}_R = [\mathbf{b}_r(\theta_1), \mathbf{b}_r(\theta_2), \dots, \mathbf{b}_r(\theta_K)] \in \mathbb{C}^{M \times K}$ and $\mathbf{B}_T = [\mathbf{b}_t(\theta_1),$

$\mathbf{b}_t(\theta_2), \dots, \mathbf{b}_t(\theta_K)] \in \mathbb{C}^{M \times K}$ denote the transmitting and receiving steering vector matrix, respectively.

In the considered model, some assumptions are made as follows.

Assumption 1: The azimuth angles of UEs are distinct and randomly distributed in $[-\frac{\pi}{2}, \frac{\pi}{2}]$.

Assumption 2: The additive white Gaussian noise is uncorrelated from the transmitted signal of the radar. In order to present the subspace, we obtain the covariance matrix of the received signal, which is given as

$$\mathbf{R}_{Y_r M \times M} = \frac{1}{L} \sum_{l=1}^L \mathbf{y}_r(l) \mathbf{y}_r^H(l) = \mathbf{\Theta} \mathbf{R}_r \mathbf{\Theta}^H + \sigma_{\omega}^2 \mathbf{I} \quad (12)$$

where $\mathbf{\Theta} = \mathbf{B}_R \text{diag}(\beta_1, \beta_2, \dots, \beta_K) \mathbf{B}_T^H$. Moreover, $\tilde{\mathbf{B}}_R$, $\tilde{\mathbf{B}}_T$ indicate the perturbed array model and the general perturbed covariance, which can be expressed as

$$\tilde{\mathbf{R}}_{Y_r} = (\mathbf{\Theta} + \tilde{\mathbf{\Theta}}) \mathbf{R}_r (\mathbf{\Theta} + \tilde{\mathbf{\Theta}})^H + \sigma_{\omega}^2 \mathbf{I} \quad (13)$$

where $\tilde{\mathbf{\Theta}} = \tilde{\mathbf{B}}_R \text{diag}(\beta_1, \beta_2, \dots, \beta_K) \tilde{\mathbf{B}}_T^H$, which contains gain errors, phase errors, sensor location errors or even mutual coupling.

According to the above assumptions, we consider the following specific types of errors.

Type 1 (Gain Errors and Phase Errors): The array response with gain and phase uncertainties $\Delta\phi_k$, $\Delta\mathbf{b}_t$ are given as follows.

$$\begin{aligned} \tilde{\mathbf{b}}_t(\phi_k) &= (|\mathbf{b}_t| + |\Delta\mathbf{b}_t|) \exp\{j(\phi_k + \Delta\phi_k)\} \\ &= |\mathbf{b}_t| e^{j\phi_k} (1 + |\Delta\mathbf{b}_t|/|\mathbf{b}_t|) e^{j\Delta\phi_k} \\ &= \mathbf{b}_t(\phi_k) + \eta_k \mathbf{b}_t(\phi_k) \end{aligned} \quad (14)$$

where the interference between each element is random and independent. In the same way, the received array response is $\tilde{\mathbf{b}}_r(\phi_k) = \mathbf{b}_r(\phi_k) + \eta_k \mathbf{b}_r(\phi_k)$, where $\phi_k = 2\pi f_0 \tau_1(\theta_k)$ and $\eta_k = (1 + |\Delta\mathbf{b}_t|/|\mathbf{b}_t|) \exp\{j\Delta\phi_k\} - 1$.

Type 2 (Mutual Coupling Errors): If spacing between antenna elements is too small or the carrier frequency is high, electromagnetic coupling effect will occur due to the interaction of space electromagnetic field. Due to the multi-input and multi-output characteristics of the MIMO radar, the mutual coupling effect between array elements cannot be ignored. For simplicity, we use the strip symmetric Toeplitz matrix \mathbf{C}_r and \mathbf{C}_t with nonzero entries to model the mutual coupling effect, which is shown as follows.

$$\tilde{\mathbf{b}}_r(\theta_k) = \mathbf{C}_r \mathbf{b}_r(\theta_k) \quad (15a)$$

$$\tilde{\mathbf{b}}_t(\theta_k) = \mathbf{C}_t \mathbf{b}_t(\theta_k) \quad (15b)$$

Type 3 (Sensor Location Errors): The array response with uncertainties caused by the deviation of the array location is indicated in the following equations.

$$\tilde{\mathbf{b}}_t(\theta_k) = [e^{-j\varphi_k^1}, \dots, e^{-j\varphi_k^M}]^T \quad (16a)$$

$$\tilde{\mathbf{b}}_r(\theta_k) = [e^{-j\varphi_k^1}, \dots, e^{-j\varphi_k^M}]^T \quad (16b)$$

where (x_m, y_m) indicates the actual sensor position and $(\Delta x_m, \Delta y_m)$ represents the error term. Moreover,

$\varphi_k^m = \frac{2\pi}{\lambda} [\tilde{x}_m \sin(\theta_k) + \tilde{y}_m \cos(\theta_k)]$, $\tilde{x}_m = x_m + \Delta x_m$ and $\tilde{y}_m = y_m + \Delta y_m$. In this case, we make an additional assumption.

Assumption 3: The sensor location error is smaller than the inter-element spacing.

All the above array disturbances will weaken the performance of AoA/AoDs estimation. To reduce the components of those disturbances, we reconstruct the received signal and estimate the number of UEs and the AoA/AoDs values in turn.

B. Path Gain Estimation With mmWave Transmitted Signals

In Equ. (2), the received signal at each time slot has a complex gain for each UE, which can be transformed to

$$\begin{aligned} \mathbf{y}_c^k[n] &= \mathbf{W}_{n,k}^H \mathbf{H}_k[n] \sum_{k=1}^K \mathbf{x}_k[n] + \mathbf{W}_{n,k}^H \mathbf{n}_k[n] \\ &= (\mathbf{x}^T[n] \otimes \mathbf{W}_{n,k}^H) \mathbf{\Lambda} \text{vec}(\mathbf{A}_{n,k}) + \mathbf{\Psi}_k[n] \end{aligned} \quad (17)$$

where $\mathbf{\Lambda} = (\mathbf{\Lambda}_{UE,k}^* \otimes \mathbf{\Lambda}_{BS,k})$. We aim to estimate the CSI of the multiuser with shorter training overhead while maintain the estimation accuracy. Path gains estimation in MIMO system starts when the UEs angle information arrives. However, orthogonal matching pursuit (OMP) based methods cannot satisfy the estimation accuracy due to the lack of measurements. Generally speaking, the estimation accuracy of LS estimator is greatly affected by noise [47]. Thus, the intelligent algorithms are applied for signal preprocessing to denoise the received signals in this paper.

Specifically, the path gain estimation process contains three sub-stages: offline training, online prediction and LS estimation, as shown in Fig. 4. In the offline training stage, a large number of previous transmitted signals and corresponding gains in the RSU buffer are used as training samples, which are used to learn the mapping function between raw and noiseless signals and to obtain the model with certain generalization performance. When the following wireless signal is received, preprocessed signals can be predicted in real time using the well-trained denoising model in the online prediction stage. Finally, the complex gains can be obtained by LS algorithm. The detailed structure of the neural network in Fig. 4 is shown in Fig. 5. The specific principle and the detailed introduction of which are given in Section IV B. Hence, time-varying mmWave channel matrix is obtained with AoA/AoDs and path gain in Equ. (9).

Note that the training and deployment of the DL estimator is at the RSU for the uplink channel conditions and the proposed channel estimation scheme can also be utilized for the downlink channel estimation with enough computing power. RSU will design the optimal beamforming vector for each user according to the prior angle information obtained by the radar module. On this base, we adopt a codebook-based beamforming scheme. For the precoder and combiner, we use the following quantized set as the candidate set $\mathbf{\Omega}$ with Q being the quantization resolution.

$$\mathbf{\Omega} = \left\{ \mathbf{a} \left(\frac{2\pi i}{2^Q} \right), i = 0, 1, \dots, 2^Q - 1 \right\} \quad (18)$$

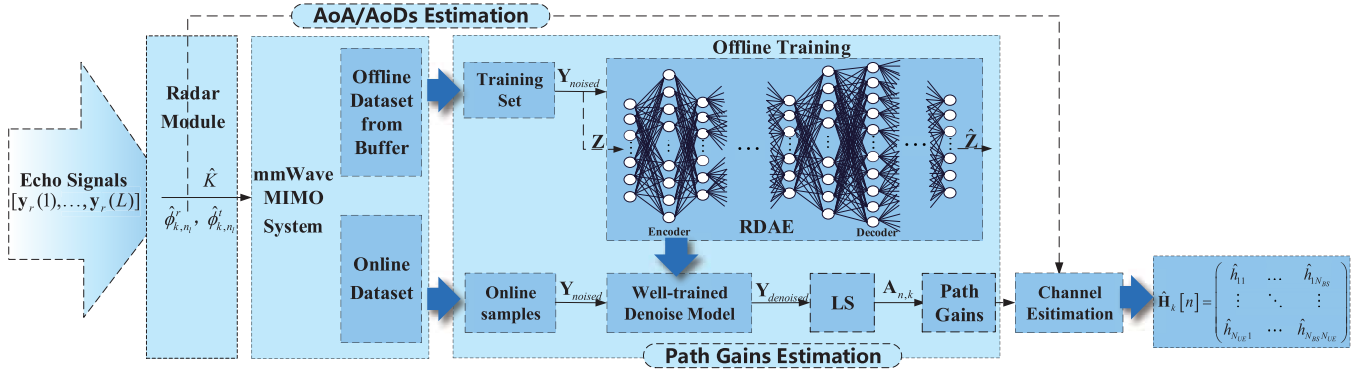


Fig. 4. Proposed scheme workflow for channel estimation.

Considering the tradeoff between performance and complexity, elements of the array response matrix are selected as the candidate set, i.e., \mathbf{a} is the steer vector. Then the beamforming vector $\mathbf{W}_{n,k}$ and $\mathbf{F}_{n,k}$ are chosen from Ω to maximize the uplink channel gain:

$$\begin{aligned} & \arg \max_{\substack{\mathbf{W}_{n,k}^H \\ \mathbf{F}_{n,k}}} \left| \mathbf{W}_{n,k}^H \mathbf{H}_k[n] \sum_{k=1}^K \mathbf{F}_{n,k} \mathbf{s}_k[n] \right| \\ \text{s.t. } & [\mathbf{F}_{n,k}]_{i,j} = \frac{1}{\sqrt{N_{UE}}} \vartheta_f, \quad \vartheta_f \in \Omega, \quad \forall i, j, \quad \forall k \\ & [\mathbf{W}_{n,k}]_{i,j} = \frac{1}{\sqrt{N_{BS}}} \vartheta_w, \quad \vartheta_w \in \Omega, \quad \forall i, j, \quad \forall k \end{aligned} \quad (19)$$

For the uplink channel, RSU's beamforming is to maximize the array gains for the incoming angles, while UEs' beamforming is to maximize the array gains for the transmitted angles. Thus, the problem can be simplified as

$$\begin{aligned} & \arg \max_{\mathbf{F}_{n,k}} \left| \mathbf{F}_{n,k}^H \mathbf{a}_{UE} \left(\hat{\phi}_{k,n_l}^t \right) \right|, \quad \forall k \\ \text{s.t. } & [\mathbf{F}_{n,k}]_{i,j} = \frac{1}{\sqrt{N_{UE}}} \varsigma_f, \quad \varsigma_f \in \left\{ \mathbf{a}_{UE} \left(\hat{\phi}_{k,n_l}^t \right) \right\}, \quad \forall k \end{aligned} \quad (20)$$

Similarly, for the RSU's combiner, we can get

$$\begin{aligned} & \arg \max_{\mathbf{W}_{n,k}} \left| \mathbf{W}_{n,k}^H \mathbf{a}_{BS} \left(\hat{\phi}_{k,n_l}^r \right) \right|, \quad \forall k \\ \text{s.t. } & [\mathbf{W}_{n,k}]_{i,j} = \frac{1}{\sqrt{N_{BS}}} \varsigma_w, \quad \varsigma_w \in \left\{ \mathbf{a}_{BS} \left(\hat{\phi}_{k,n_l}^r \right) \right\}, \quad \forall k \end{aligned} \quad (21)$$

In summary, the optimal precoding vectors will be found by searching in all possible cases of the array response.

IV. MIMO RADAR AIDED TIME-VARYING MMWAVE CHANNEL ESTIMATION ALGORITHM

A. Subspace Reconstruction Based AoA/AoDs Estimation

As shown in Equ. (13), the covariance matrix of the signal is no longer a standard form due to the considered errors of the arrays. The classic MUSIC algorithm [48] works by constructing spatial spectral function and finding the angles at peaks with perfect arrays. However, the actual array manifold inevitably deviates from the nominal one due to array

uncertainties in practical applications, which will result in not strictly orthogonal relationship between the signal subspace of the actual received data and the nominal array manifold. When the deviation is large, the angle estimation performance of the subspace algorithms like MUSIC may be unavailable. Therefore, a novel subspace decomposition based AoA/AoDs estimation method named two-step angle estimation (TSAE) algorithm is proposed in this subsection.

In Equ. (13), the eigenvalue decomposition of the perturbed covariance $\tilde{\mathbf{R}}_{Y_r}$ is performed as follows.

$$\begin{aligned} \tilde{\mathbf{R}}_{Y_r, M \times M} &= \sum_{i=1}^M \lambda_i \mathbf{u}_i (\mathbf{u}_i)^H \\ &= \mathbf{U}_r \mathbf{V}_r (\mathbf{U}_r)^H + \sigma_{\tilde{\omega}}^2 \mathbf{U}_n (\mathbf{U}_n)^H \end{aligned} \quad (22)$$

where the eigenvalues in descending order is $\lambda_1 \geq \dots \geq \lambda_K \geq \lambda_{K+1} \geq \dots \geq \lambda_M \geq \sigma_{\tilde{\omega}}^2$. $\mathbf{U}_r = [\mathbf{u}_1, \mathbf{u}_2, \dots, \mathbf{u}_K]$ and $\mathbf{U}_n = [\mathbf{u}_{K+1}, \mathbf{u}_{K+2}, \dots, \mathbf{u}_M]$ denote the eigenvectors that constitute the subspace of signal and noise, respectively. The degree of difference between adjacent eigenvalues can be expressed as a ratio variable as follows.

$$\mu_k = \lambda_k / \lambda_{k+1}, \quad k = 1, 2, \dots, M-1 \quad (23)$$

Obviously, when the variable reach the maximum, the corresponding k is the number of the main eigenvalues. Therefore, we can get the estimated number of targets \hat{K} at

$$\hat{K} = \arg \max_{k=1, 2, \dots, M-1} [\mu_k] \quad (24)$$

Through (24), the eigenvectors with the largest eigenvalues are taken as the dominant features and the retained data will have no correlation in each orthogonal direction. We project the perturbed signal $\tilde{\mathbf{Y}}$ into a transformed space with N_P ($N_P < M$) vectors $\mathbf{U}_P = [\mathbf{u}_1, \mathbf{u}_2, \dots, \mathbf{u}_{N_P}]_{M \times N_P}$ through $\mathbf{Y}_P = \tilde{\mathbf{Y}} \mathbf{U}_P$, retaining the main components and discarding the parts with noise and array errors to a certain extent. The new covariance matrix can be expressed as

$$\mathbf{R}_P = \mathbf{Y}_P \mathbf{Y}_P^H / N_P \quad (25)$$

This completes the subspace reconstruction of the signal. Note that \hat{K} and equation (25) can be regarded as known parameters and the vehicle azimuth angles can be obtained by finding roots. Specifically, we get the new eigenvalues

Algorithm 1 Two-Step Angle Estimation (TSAE) Algorithm for mmWave AoA/AoDs Estimation in MU-MIMO V2X Communications

Input: Received signal of MIMO radar $\tilde{\mathbf{R}}_{Y_r}$, number of primary features reserved N_P .

Output: Number of UEs \hat{K} , AoA/AoDs: ϕ^t and ϕ^r .

- 1: Perform eigenvalue decomposition of $\tilde{\mathbf{R}}_{Y_r}$ as Equ. (22).
- 2: Sort the eigenvalues in descending order as $\lambda_1 \geq \dots \geq \lambda_K \geq \lambda_{K+1} \geq \dots \geq \lambda_M \geq \sigma_{\tilde{\omega}}^2$.
- 3: Calculate the ratio variable according to Equ. (23).
- 4: Obtain \hat{K} according to Equ. (24).
- 5: Obtain $\mathbf{U}_P = [\mathbf{u}_1, \mathbf{u}_2, \dots, \mathbf{u}_{N_P}]$.
- 6: Project the signal into a transformed space by $\mathbf{Y}_P = \tilde{\mathbf{Y}}\mathbf{U}_P$.
- 7: Perform the second eigenvalue decomposition as Equ. (26).
- 8: Construct the polynomial and find roots according to Equ. (27)(28).
- 9: **return** \hat{K} , the roots ϕ^t and ϕ^r .

$\eta_1 \geq \dots \geq \eta_K \geq \eta_{K+1} \geq \dots \geq \eta_M$ and the eigenvectors $\mathbf{U} = [\tilde{\mathbf{U}}_r, \tilde{\mathbf{U}}_n]$ through the second eigenvalue decomposition of \mathbf{R}_P , which is indicated as follows.

$$\mathbf{R}_P = \sum_{i=1}^M \eta_i \tilde{\mathbf{u}}_i (\tilde{\mathbf{u}}_i)^H = \tilde{\mathbf{U}}_r \tilde{\mathbf{V}}_r (\tilde{\mathbf{U}}_r)^H + \tilde{\sigma}_{\tilde{\omega}}^2 \tilde{\mathbf{U}}_n (\tilde{\mathbf{U}}_n)^H \quad (26)$$

We can express the signal space in this way [49].

$$\mathbf{c} = \mathbf{U}_{n1} (\mathbf{U}_{n2})^{-1} [1, 0, \dots, 0]^T \in \mathbb{C}^{(M-\hat{K}) \times 1} \quad (27)$$

where $\mathbf{c} = [c_1, c_2, \dots, c_{M-\hat{K}}]$. After recombining the polynomial referring to [49], the polynomial can be constructed as

$$f(z) = \sum_{i=1}^{\hat{K}+1} c_i z^{i-1}, \quad c_{\hat{K}+1} = 1 \quad (28a)$$

$$z_i = \exp(j\omega_i), \quad 1 \leq i \leq \hat{K} \quad (28b)$$

Then we can get the roots of Equ. (28), which are the estimated AoA/AoDs ϕ^t and ϕ^r . Obviously, our algorithm calculate the angle value by rooting instead of the angle quantization and grid matching. Hence, no quantization error will be introduced.

B. DL Based Path Gains Estimation

The RSU conducts beamforming according to the estimated AoA/AoDs, and thereby the signal can be simplified by ignoring the combiner temporarily, which is given by

$$\begin{aligned} \mathbf{Z}_c^k[n] &= \mathbf{W}_{n,k} \mathbf{y}_c^k[n] / \mathbf{W}_{n,k} \mathbf{W}_{n,k}^H \\ &= \mathbf{H}_k[n] \sum_{k=1}^K \mathbf{x}_k[n] + \mathbf{n}_k[n] \\ &= (\mathbf{x}^T[n] \otimes \mathbf{I}) \mathbf{A} \text{vec}(\mathbf{A}_{n,k}) + \mathbf{n}_k[n] \end{aligned} \quad (29)$$

which will be denoised by the neural network.

1) *Main Idea:* The gain estimation consists of offline training and online estimation as shown in Fig. 4. For the sake of saving pilot overhead, model training will be executed offline. The vehicles transmit pilot signals to the RSU. Simultaneously, the MIMO radar continuously sends detection signals within a certain range. When the radar receives the echo reflected from the target vehicle, the angle estimation is conducted and the angle information is transmitted to the communication module, which determines the optimal beamforming to prepare for the downlink transmission. During this phase, RSU buffer stores a large amount of wireless signals \mathbf{Y}_{noised} and $\mathbf{Y}_{denoised}$ as the training set for RDAE training. After the derivation of Equ. (29), we obtain the input data \mathbf{Z} of the training stage. Benefit from the AoA/AoDs from MIMO radar, the data in training set has the known angle information, which means the steer vectors $\mathbf{\Lambda}$ are known. The well-trained model ‘‘RDAE’’ can be obtained by limited iterations. In the online estimation stage, the mmWave MIMO system inputs real-time signals into the model and the network output $\hat{\mathbf{Z}}$ is the denoised data. Assuming that the weight vector of RDAE is \mathbf{w} and the mapping relation between input and output can be expressed as

$$\hat{\mathbf{Z}} = \mathcal{F}(\mathbf{Z}; \mathbf{w}) = \mathcal{F}^{(n-1)} \left(\mathcal{F}^{(n-2)} \left(\dots \mathcal{F}^{(1)}(\mathbf{Z}) \right) \right) \quad (30)$$

The network is trained end-to-end according to the loss function, which is given by

$$\text{loss} = \frac{1}{N_{sa}} \sum_{i=1}^{N_{sa}} \left\| \hat{\mathbf{Z}}_i - \mathbf{Z}_i \right\|_2^2 \quad (31)$$

where $\|\cdot\|_2$ means the euclidean norm and N_{sa} is the number of the training data.

The network will stop training when the loss function stops falling and then a well-trained denoising model is constructed. The well-trained model can accomplish online denoising within fewer pilots and further achieve gain calculation using LS algorithm, which is given by

$$\begin{aligned} (\hat{\mathbf{A}}_{n,k})_i &= \arg \min_{(\mathbf{A}_{n,k})_i} \left\| \hat{\mathbf{Z}}_c^k[n] - \mathbf{\Gamma}_{n,i} \text{vec}(\hat{\mathbf{A}}_{n,k})_i \right\|_2 \\ &= \left(\mathbf{\Gamma}_{n,i}^H \mathbf{\Gamma}_{n,i} \right)^{-1} \mathbf{\Gamma}_{n,i}^H \left(\hat{\mathbf{Z}}_c^k[n] \right)_i \end{aligned} \quad (32)$$

where \mathbf{Z}_c^k after removing noise is $\hat{\mathbf{Z}}_c^k$ and $\mathbf{\Gamma}_n = (\mathbf{x}^T[n] \otimes \mathbf{I}) \mathbf{\Lambda}$.

2) *RDAE Model:* The core idea of DAE is to encode and decode the original data corrupted by the noise, and finally the network outputs the recovered data without noise. The initial DAE first adds noise to input data satisfying a certain distribution as training data.

In this subsection, we propose a path gains estimation method based on angle priori. We introduce residual learning into DAE and propose a learning framework with residual structure for wireless gain estimation, named RDAE. The stucture of RDAE is shown in Fig. 5. The size of $\mathbf{Z}_c^k[n]$ is $N_{BS} \times 1$ and the total data matrix size is $2 \times K \times N_{BS} \times C_G$ (complex value is split into real and imaginary part), which can be written as

$$\mathbf{Z}_c = [\text{Re}(\mathbf{Z}_c), \text{Im}(\mathbf{Z}_c)] \quad (33)$$

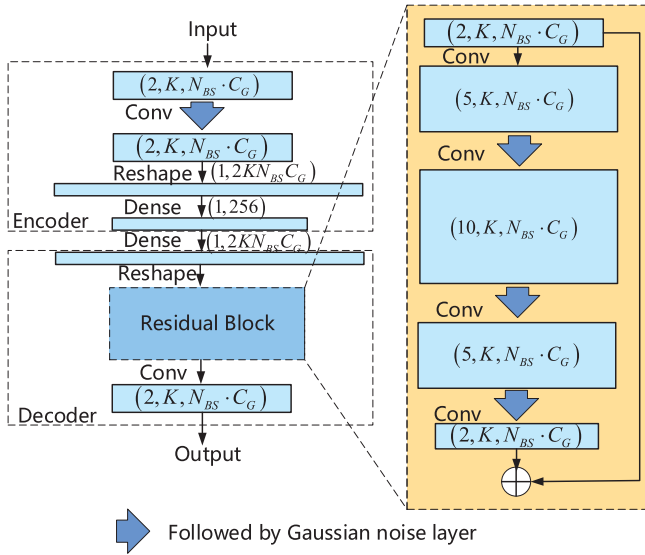


Fig. 5. Proposed RDAE learning framework design.

To adjust to the input size of the network, we transform the dimension of the data matrix as $2 \times K \times N_{BS}C_G$, which is the input size of the network. The size of all convolution kernels used in RDAE is 3×3 . Furthermore, the activation function of each convolutional layer is “Leaky ReLU”, and the fully connected layer exists without nonlinear activation. RDAE can be coarsely divided into the encoder and decoder part. In the encoder, the first layer is a convolutional layer with 2 filters, which maps the input to output of size $2 \times K \times N_{BS}C_G$. In particular, we have added a layer of Gaussian noise as a scrambling to the training signal. Then we vectorize the signal through “Reshape”. The following layer is the fully connected layer, which encodes the data to 256 bits as the input of the decoder. In the decoder part, the first layer of the decoder is a dense layer, which converts the encoded vector to the previous length. The dense layer can be regarded as the first layer decoding of the codebook. Next to the dense layer is the Residual blocks, where each block consists of 4 convolutional layers. The last layer has 2 filters and the size of the whole output is the same as the input. Except for the first layer, there is a Gaussian layer after each layer, which is used to descramble the data’s own noise and the artificially added noise. Note that the Gaussian Noise layer also plays a role of regularization, which is beneficial to avoid overfitting problem.

Assuming that the noise follows the complex Gaussian distribution, we choose “RandomNormal” for the weight initialization to assist the Gaussian noise layer and guide the network to converge faster.

V. PERFORMANCE ANALYSIS

In this section, we analyze the performance of the proposed channel estimation scheme, including the derivation of Cramer-Rao lower bounds of channel estimation and the computational complexity of each algorithm.

A. Cramer-Rao Lower Bound Analysis

CRLB theoretically provides the maximum estimation accuracy available for the unbiased estimation, which acts as

Algorithm 2 DL Based Path Gain Estimation Algorithm in MU-MIMO V2X Communications

Input: Transmitted signals \mathbf{y}_c from UEs, estimated AoA/AoDs and well-trained RDAE.

Output: Path gains $\hat{\mathbf{A}}$ and channel matrix $\hat{\mathbf{H}}$.

- 1: Load the RDAE which has been well trained.
- 2: Preprocess the signals by Equ. (29)(33).
- 3: Process the RDAE.
- 4: Update the output $\hat{\mathbf{Z}}$ by Equ. (30).
- 5: Calculate the output $\hat{\mathbf{A}}_{n,k}$ according to Equ. (32).
- 6: Obtain $\hat{\mathbf{H}}_k[n]$ according to Equ. (9).
- 7: **return** $\hat{\mathbf{A}}$ and $\hat{\mathbf{H}}$.

an upper bound for the performance of the estimation method.

In the stage of path gains estimation, we derive the lower bound of estimation error with the signal model given in Equ. (17). The noise $\mathbf{n}_k[n]$ follows the complex Gaussian distribution $\mathcal{CN}(\mathbf{0}_{N_{BS} \times 1}, \sigma_n^2 \mathbf{I}_{N_{BS}})$. Let $\Xi_k = (\mathbf{x}^T[n] \otimes \mathbf{W}_{n,k}^H) \mathbf{A}$. Thus, the conditional probability density function [50] of y_c with the given path gains matrix \mathbf{A} is

$$p_{y_c|\mathbf{A}}(y_c; \mathbf{A}) = \frac{1}{(2\pi\sigma_n^2)^{N_L/2}} \exp\left\{-\frac{1}{2\sigma_n^2} \|y_c - \Xi\mathbf{A}\|_2^2\right\} \quad (34)$$

For simplicity, we neglected the number of UEs. Then we obtain the CRLB of path gain estimation [18], which is given as follows.

$$\mathbb{E}\left[\|\hat{\mathbf{A}} - \mathbf{A}\|_2^2\right] \geq \sigma_n^2 \cdot N_L^2 / \text{tr}\left\{\left(\Xi^H \Xi\right)\right\} = \text{CRLB}(\mathbf{A}) \quad (35)$$

Based on (35), we give the performance upper bound of channel matrix estimation with known targets angle information. The MSE of the channel estimation can be expressed as

$$\mathbb{E}\left[\|\hat{\mathbf{H}} - \mathbf{H}\|_F^2\right] \geq \frac{\xi_{\min} \sigma_n^2 N_L^2}{\text{tr}\left\{\left(\Xi^H \Xi\right)\right\}} = \text{CRLB}(\mathbf{H}) \quad (36)$$

where ξ_{\min} denotes the minimum eigenvalue of matrix $\mathfrak{B}^H \mathfrak{B}$. \mathfrak{B} equals to $\Lambda_{UE,k}^* \odot \Lambda_{BS,k}$, where \odot means Khatri-Rao product. The derivation is given in Appendix B in detail.

B. Computational Complexity Analysis

The computational complexity in the entire channel estimation scheme comes from the following two stages:

- For the stage of AoA/AoDs estimation, the computational complexity mainly comes from the EVD and polynomial rooting. In this stage, $\mathcal{O}_c(\cdot)$ indicates the number of complex multiplications. Calculating the covariance matrix of the signal requires $\mathcal{O}_c(M^2L)$ complex multiplications. The complexity of EVD is $\mathcal{O}_c(M^3)$ and it takes $\mathcal{O}_c(M-1)$ complex divisions to search the number of targets. Then, subspace reconstruction requires $\mathcal{O}_c(MLN_P)$ complex multiplications

($M > N_P$). Similarly, to obtain the transformed covariance matrix needs $\mathcal{O}_c(M^2 N_P)$ complex multiplications. The complexity of the final EVD and root finding is $\mathcal{O}_c(M^3)$ and $\mathcal{O}_c((M-1)^3)$, respectively. Therefore, the total computational complexity of angle estimation is $\mathcal{O}_c(M^3 + M^2 L)$.

- For the stage of path gains estimation, the computational originates from the CNN processing for signal denoising and the complexity of the LS, which can be negligible compared to the former. Note that $\mathcal{O}_f(\cdot)$ in this stage represents the time complexity, i.e., floating-point operations. If the size of the output feature map is $h_o \times h_o$, the size of the convolution kernel is $h_k \times h_k$, and the number of input and output channels is n_{in} and n_{out} , then the time complexity of a single convolutional layer is $\mathcal{O}_f(h_o^2 \cdot h_k^2 \cdot n_{in} \cdot n_{out})$ without bias. The complexity of a single dense layer is $\mathcal{O}_f(h_{in}^2 \cdot n_{in} \cdot n_{out})$, where h_{in} is the input feature size. Hence, the complexity of the entire RDAE is $\mathcal{O}_f\left(\sum_{i=1}^D h_{oi}^2 \cdot h_{ki}^2 \cdot n_{i-1} \cdot n_i\right)$, where D is the depth of the CNN and n_i is the output channels of the i th layer. Specifically, $h_{oi} = 1$ and $h_{ki} = h_{o(i-1)}$ for dense layers.

VI. SIMULATIONS

In this section, we will further analyze the previous discussion through simulations and compare the performance of the proposed scheme under different conditions. This section contains three parts: the AoA/AoDs estimation, the path gains estimation and the channel estimation. The simulation settings are set as follows.

Uplink transmission frame structure: $T_s = 1\mu s$ and the number of pilots are $P_1 = C_I = L = 100$, $C_G = 5$ and $C_D = 65$, respectively.

MIMO radar module: The transmitting and receiving arrays of the radar are equipped with $M = 24$. There are four uncorrelated UEs with $\theta_1 = -\pi/6$ rad, $\theta_2 = -\pi/18$ rad, $\theta_3 = \pi/9$ rad and $\theta_4 = 2\pi/9$ rad in the current channel, respectively.

Communication module: $f_{mW} = 90$ GHz and $N_{BS} = 16$.

The proposed DL-based algorithm is implemented on a computer with an Intel(R) Xeon(R) CPU E5-2630 v3 @ 2.40GHz CPU, a NVIDIA GeForce GTX 1080 GPU and 16GB memory. Tensorflow 1.5.0 and python 3.5 are used for the estimation.

A. AoA/AoDs Estimation Performance

In this subsection, we show the performance of subspace reconstruction based angle estimation algorithm with MIMO radar in time-varying mmWave channels in detail. We take $N_P = M - 2$ in the simulation. Fig. 6 and Fig. 7 are experimented under the conditions of $\Delta\phi_k = \mathcal{N}(0, \sqrt{0.1})$, $\Delta\mathbf{b}_t = \mathcal{N}(1.0, \sqrt{0.1})$ and $(\Delta x_m, \Delta y_m) = \mathcal{N}(0, \sqrt{0.01d_{mW}})$. The resolution probability of AoA/AoDs under strict condition¹

¹In the case that two UEs are $\theta_1 = -\delta$ deg and $\theta_2 = \delta$ deg respectively, it is regarded as a successful resolution if $-\delta \leq \theta_2 < 0$ and $0 < \theta_2 \leq \delta$.

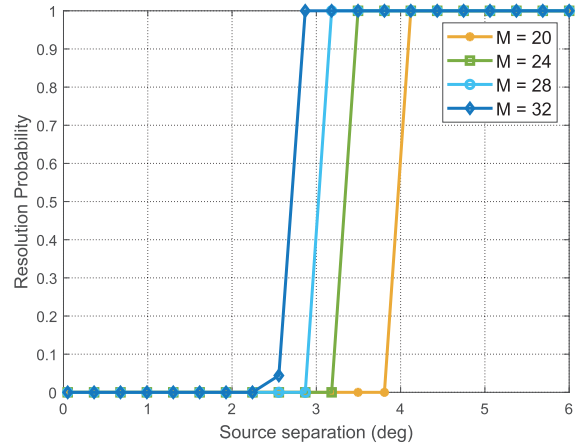


Fig. 6. Resolution probability of AoA/AoDs.

in Fig. 6, which requires the estimated angles are reasonably close to the correct ones. As the number of antennas increases, the resolution probability of the algorithm becomes more precise and reaches 100% when source separation is 2.9 degree equipped with 32 elements.

We define the RMSE to measure the AoA/AoDs estimation performance

$$\text{RMSE}_{\text{AoA/AoDs}} = 10 \lg \sqrt{\frac{1}{K} \frac{1}{N_{mc}} E \left[\sum_{n=1}^{N_{mc}} \sum_{k=1}^K \left\| \theta_k - \hat{\theta}_k \right\|_2^2 \right]} \quad (37)$$

where N_{mc} is the number of Monte-Carlo experiments and it equals to 3000. The curves in Fig. 7 show the RMSE of sparse recovery, ESPRIT, MVDR, root MUSIC and the proposed algorithm. It can be seen that the estimation performance fluctuates slightly with the change of SNR due to the signal subspace is reconstructed twice and most of the noise components are removed. Therefore the increase of SNR performs slight impact on the accuracy of the estimation algorithms. However, the performance differences between the algorithms are significant. Root MUSIC and the proposed scheme have the better performance than the other three experiments. Especially, our proposed algorithm is more superior because other algorithms have a sharp deterioration in performance due to severe non-orthogonality.

Compared with other array errors, the correction of array mutual coupling errors is more complex. From Fig. 8, we can find that our approach has about 0.6dB improvement over conventional root MUSIC with 16 elements and $p_M = 3$ due to the enhancement of the orthogonality, where the mutual coefficient is $[1, 0.4146 + 0.4537j, 0.4489 + 0.4167j]$.

B. Path Gains Estimation Performance

In the following simulations, 35000 wireless signals are generated, 25000 for training, 5000 for validation and 5000 for testing. Moreover, the training batch size is set as 256.

The proposed RDAE gain estimator is compared with LS estimator, Refined estimator [51], and DAE estimator. The performance comparison without the Doppler frequency

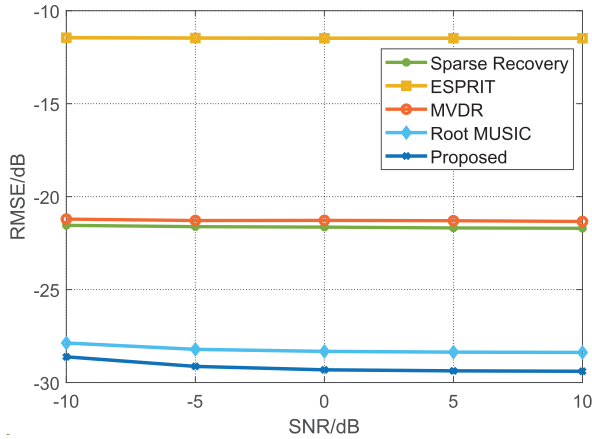


Fig. 7. RMSE performance of AoA/AoDs against SNR.

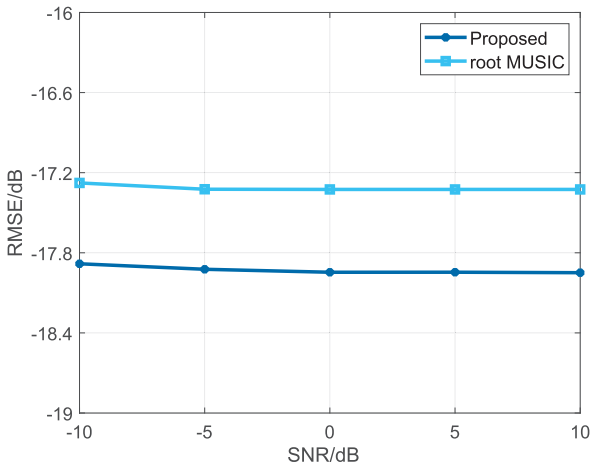


Fig. 8. RMSE performance of AoA/AoDs of mutual coupling against SNR.

shift is illustrated in Fig. 9. The transmitter and receiver are equipped with 8×16 array elements respectively. The angle values in the samples are the results of the previous MIMO radar angle estimation scheme, rather than relying on the assumed perfect angle. Refer to the CRLB derived above, it is obvious that RDAE achieves the best performance within the testing SNR range. LS is the worst when SNR is lower than 5dB due to not considering the influence of the noise. For the same problem, different network structures may also cause differences in estimated performance. Clearly, DAE greatly reduces its learning ability and it basically has no ability to denoise due to the lack of residual learning module.

Compared with the other two comparison methods, the “Refined” has a certain performance improvement, its main idea is that rough channel gains are calculated by LS and then used as input to obtain more accurate gains through further optimization of RDAE. However, the difference between the low-resolution complex gains directly estimated by LS and the more accurate high-resolution gains is not simple noise interference, the learning difficulty of which is undoubtedly higher than the denoising operation of the signal for the DL estimator. The above results can prove that RDAE is more adaptable to high-mobility time-varying channels and has higher estimation accuracy.

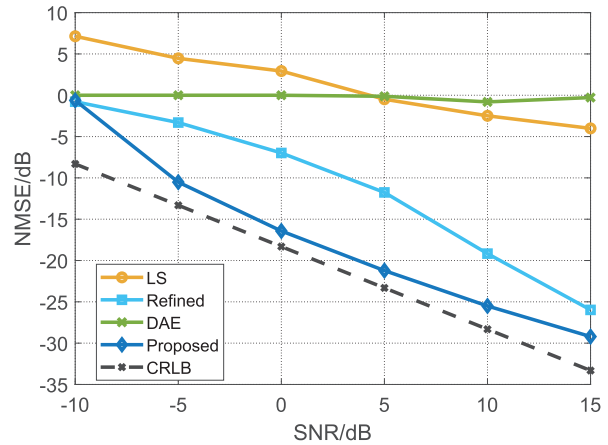


Fig. 9. NMSE performance comparison of path gains estimation against SNR.

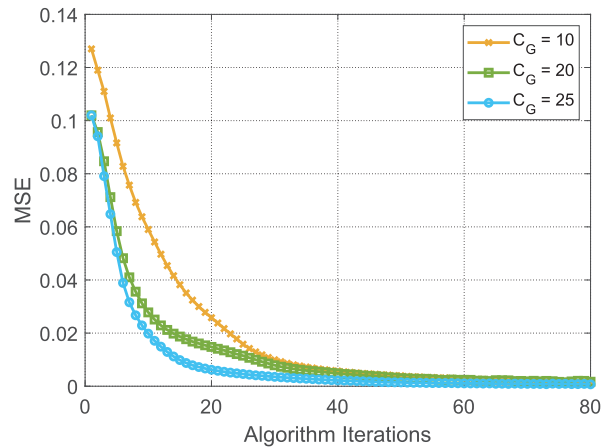


Fig. 10. Comparison of algorithm convergence under different number of training pilots.

The fast convergence of the proposed RDAE within different training lengths $C_G = 10, 15, 25$ is illustrated in Fig. 10. It is shown that the network has basically completed convergence at the 60-th epoch and the loss of the network at this point is close to zero for all C_G values due to the low difficulty for the network to learn the mapping between the input and the output. From the beginning to the 40-th epoch, the loss decreases more rapidly when the C_G is larger, which is indicated that it has more information to guide learning.

In order to visualize the impact of vehicle speed on the performance of the algorithm, we give the estimated error curves of the algorithm in Fig. 11 with the normalized Doppler frequency shift from 0 to 0.2, that is, the moving speed of the vehicle ranges from 0 km/h to 144 km/h. The SNR is set from -5 dB to 15dB. In Fig. 11, it is shown that the NMSE increases monotonically with the frequency shift and this trend becomes more obvious as the SNR increases. However, the curve rises very slowly, which means that our gain estimator is robust to Doppler frequency shift.

C. Channel Estimation Performance

To confirm the performance of our proposed channel estimation scheme based on angle prior, Fig. 12 depicts the channel

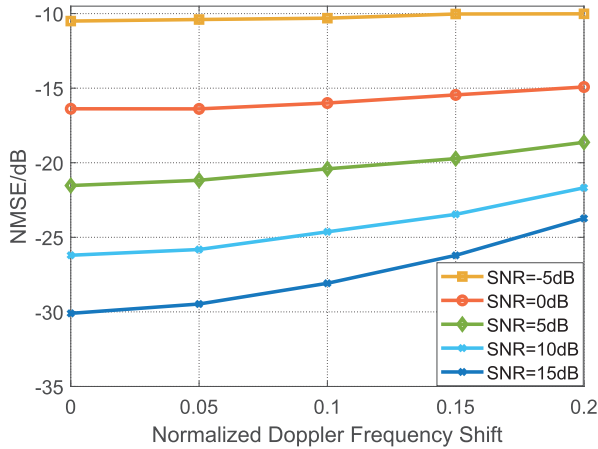


Fig. 11. NMSE performance of path gains estimation against normalized Doppler frequency shift.

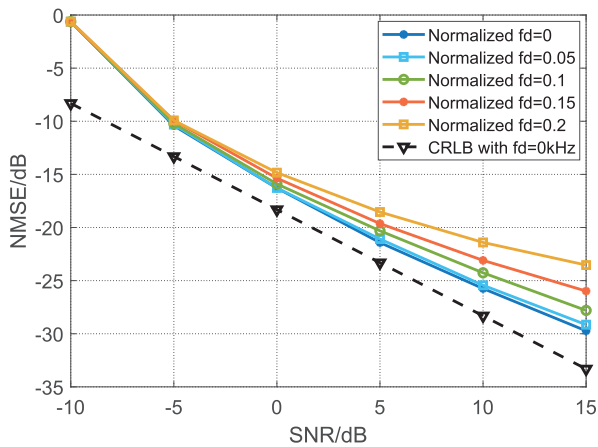


Fig. 12. NMSE performance of channel estimation against SNR.

estimation performance curves and CRLB under static conditions. When the SNR is above -5 dB, the user mobility causes the curves to gradually deviate from the CRLB. However, the result indicates that the NMSE deviation is only about 5 dB even when the vehicle is driving at the highest speed, which proves that the proposed scheme is highly adaptable to frequency shift once again.

VII. CONCLUSION

In this paper, a novel uplink channel estimation scheme for the mmWave MU-MIMO system over a time-varying channel is proposed. Specially, we proposed a novel transmission frame structure including communication and radar modules, where the channel estimation is decomposed into AoA/AoDs estimation with MIMO radar and channel gain estimation. In the first stage, MIMO radar are equipped for channel angle estimation, where the echo signal was reconstructed and the reconstructed covariance matrix was used for channel angle estimation with short training resources. On the basis of the estimated AoA/AoDs, a DL-based path gain estimator were leveraged to learn the mapping relationship between the raw data and the noised data, which was leveraged to optimize the performance of gain estimation. The performance of the proposed algorithms is evaluated and analyzed under the

single-path MU-MIMO channel case in high-mobility V2X scenarios. The simulation results demonstrated that our proposed scheme estimated the time-varying mmWave channels effectively when vehicles are moving at high speed.

APPENDIX A

PROOF OF THE RATIONALITY OF USING MIMO RADAR

For monostatic radar, if the distance between the target and the radar is R_{LoS} , the time required for the radar detection wave to travel back and forth between the radar and the target is T_{LoS} , where c is the speed of light.

$$T_{LoS} = 2R_{LoS}/c \quad (38)$$

Assuming that the maximum LoS distance R_{LoS} is 600 meters and the RSU's height R_h is 100 meters, the upper limit of the time required for radar detection is $4 \mu s$. As shown in Fig. 1, the change in angle for vehicle k during the observation interval ΔT is $\Delta\theta_k$ is

$$\Delta\theta_k = |\theta_k^2 - \theta_k^1| \leq \arctan(R_\Delta/R_h) \quad (39)$$

where R_Δ is the vehicle moving distance during the observation period, and R_h is the vertical height of the RSU. Therefore, if the vehicle moving speed is V_{UE} , then

$$R_\Delta = V_{UE}\Delta T \quad (40)$$

We set the target angle to be constant when the angle difference is less than 2° . Then the following inequality can be obtained.

$$\Delta\theta_k \leq \arctan(R_\Delta/R_h) = \arctan(V_{UE}\Delta T/R_h) \leq \pi/180 \quad (41)$$

According to $\tan \xi \approx \xi$ when $\xi \approx 0^\circ$, it can be derived that

$$\Delta T \leq \pi R_h/180V_{UE} \quad (42)$$

If the vehicle speed is 120 km/h, then $\Delta T \approx 0.0524 s$, i.e., 5.24×10^4 pilots. Obviously, $\Delta T > P_1 T_s$, which is indicated that the target angle can be regarded as unchanged during the radar detection of the target position and the AoA/AoDs training period.

APPENDIX B

PROOF OF THE CRLB

The fisher information matrix (FIM) [50] can be denoted as

$$\mathbf{F}(\mathbf{A}) \stackrel{def}{=} -E \left\{ \frac{\partial^2 \ln p_{y_c|\mathbf{A}}(y_c; \mathbf{A})}{\partial \mathbf{A}_i \partial \mathbf{A}_j} \right\} = \frac{1}{\sigma_n^2} [\boldsymbol{\Xi}^H \boldsymbol{\Xi}]_{i,j} \quad (43)$$

According to the vector estimation theory [18], we have $\text{CRLB}(\mathbf{A}) = \text{tr} \{ \mathbf{F}(\mathbf{A})^{-1} \} = \sigma_n^2 \text{tr} \{ (\boldsymbol{\Xi}^H \boldsymbol{\Xi})^{-1} \}$, where

$$\begin{aligned} \text{tr} \{ (\boldsymbol{\Xi}^H \boldsymbol{\Xi})^{-1} \} &= \sum_{n_l=1}^{N_L} \lambda_{n_l}^{-1} = N_L \left[\frac{1}{N_L} \sum_{n_l=1}^{N_L} \lambda_{n_l}^{-1} \right] \\ &\stackrel{(q)}{\geq} N_L \left(N_L / \sum_{n_l=1}^{N_L} \lambda_{n_l} \right) \\ &= N_L^2 / \text{tr} \{ (\boldsymbol{\Xi}^H \boldsymbol{\Xi}) \} \end{aligned} \quad (44)$$

λ_{n_l} denotes the n_l th eigenvalue of $\Xi^H \Xi$ and the basis of (q) is arithmetic-harmonic means inequality. Based on this, we can further obtain the CRLB of the channel matrix [18], which is given as follows.

$$\begin{aligned} \mathbb{E} \left[\left\| \hat{\mathbf{H}} - \mathbf{H} \right\|_F^2 \right] &= \mathbb{E} \left[\left\| (\Lambda_{UE}^* \odot \Lambda_{BS}) (\hat{\mathbf{A}} - \mathbf{A}) \right\|_2^2 \right] \\ &\geq \xi_{\min} \mathbb{E} \left[\left\| \hat{\mathbf{A}} - \mathbf{A} \right\|_2^2 \right] \\ &= \frac{\xi_{\min} \sigma_n^2 N_L^2}{\text{tr} \left\{ \left(\Xi^H \Xi \right) \right\}} \end{aligned} \quad (45)$$

REFERENCES

- [1] F. Boccardi, R. W. Heath, A. Lozano, T. L. Marzetta, and P. Popovski, "Five disruptive technology directions for 5G," *IEEE Commun. Mag.*, vol. 52, no. 2, pp. 74–80, Feb. 2014.
- [2] M. Shafi *et al.*, "5G: A tutorial overview of standards, trials, challenges, deployment, and practice," *IEEE J. Sel. Areas Commun.*, vol. 35, no. 6, pp. 1201–1221, Jun. 2017.
- [3] A. N. Uwaechia and N. M. Mahyuddin, "A comprehensive survey on millimeter wave communications for fifth-generation wireless networks: Feasibility and challenges," *IEEE Access*, vol. 8, pp. 62367–62414, 2020.
- [4] T. S. Rappaport, Y. Xing, G. R. MacCartney, A. F. Molisch, E. Mellios, and J. Zhang, "Overview of millimeter wave communications for fifth-generation (5G) wireless networks—With a focus on propagation models," *IEEE Trans. Antennas Propag.*, vol. 65, no. 12, pp. 6213–6230, Dec. 2017.
- [5] T. S. Rappaport *et al.*, "Millimeter wave mobile communications for 5G cellular: It will work!," *IEEE Access*, vol. 1, pp. 335–349, 2013.
- [6] Z. Pi and F. Khan, "An introduction to millimeter-wave mobile broadband systems," *IEEE Commun. Mag.*, vol. 49, no. 6, pp. 101–107, Jun. 2011.
- [7] M. A. Abu-Rgheff, "Millimetre wave massive MIMO technology," in *5G Physical Layer Technologies*. Hoboken, NJ, USA: Wiley, 2020.
- [8] Y. Deng, L. Wang, K.-K. Wong, A. Nallanathan, M. Elkashlan, and S. Lambotharan, "Safeguarding massive MIMO aided hetnets using physical layer security," in *Proc. Int. Conf. Wireless Commun. Signal Process. (WCSP)*, Oct. 2015, pp. 1–5.
- [9] K. M. S. Huq and J. Rodriguez, "Backhauling 5G small cells with massive-MIMO-enabled mmWave communication," in *Backhauling/Fronthauling for Future Wireless Systems*. Hoboken, NJ, USA: Wiley, 2017.
- [10] *Telecommunications and Exchange Between Information Technology Systems—Requirements for Local and Metropolitan Area Networks—Part 11: Wireless LAN Medium Access Control (MAC) and Physical Layer (PHY) Specifications—Amendment 3: Enhancements for Very High Throughput to Support Chinese Millimeter Wave Frequency Bands (60 GHz and 45 GHz)*, Standard ISO/IEC/IEEE 8802-11:2018/Amd.3:2020(E), 2020, pp. 1–310.
- [11] A. Alkhateeb, J. Mo, N. Gonzalez-Prelcic, and R. W. Heath, "MIMO precoding and combining solutions for millimeter-wave systems," *IEEE Commun. Mag.*, vol. 52, no. 12, pp. 122–131, Dec. 2014.
- [12] C. Hu, L. Dai, T. Mir, Z. Gao, and J. Fang, "Super-resolution channel estimation for mmWave massive MIMO with hybrid precoding," *IEEE Trans. Veh. Technol.*, vol. 67, no. 9, pp. 8954–8958, Sep. 2018.
- [13] J. Lee, G.-T. Gil, and Y. H. Lee, "Channel estimation via orthogonal matching pursuit for hybrid MIMO systems in millimeter wave communications," *IEEE Trans. Commun.*, vol. 64, no. 6, pp. 2370–2386, Jun. 2016.
- [14] Z. Gao, L. Dai, Z. Wang, and S. Chen, "Spatially common sparsity based adaptive channel estimation and feedback for FDD massive MIMO," *IEEE Trans. Signal Process.*, vol. 63, no. 23, pp. 6169–6183, Dec. 2015.
- [15] A. Alkhateeb, O. E. Ayach, G. Leus, and R. W. Heath, "Channel estimation and hybrid precoding for millimeter wave cellular systems," *IEEE J. Sel. Topics Signal Process.*, vol. 8, no. 5, pp. 831–846, Oct. 2014.
- [16] W. Zhang, W. Zhang, and J. Wu, "UAV beam alignment for highly mobile millimeter wave communications," *IEEE Trans. Veh. Technol.*, vol. 69, no. 8, pp. 8577–8585, Aug. 2020.
- [17] K. Guan *et al.*, "Towards realistic high-speed train channels at 5G millimeter-wave band—Part I: Paradigm, significance analysis, and scenario reconstruction," *IEEE Trans. Veh. Technol.*, vol. 67, no. 10, pp. 9112–9128, Oct. 2018.
- [18] Q. Qin, L. Gui, P. Cheng, and B. Gong, "Time-varying channel estimation for millimeter wave multiuser MIMO systems," *IEEE Trans. Veh. Technol.*, vol. 67, no. 10, pp. 9435–9448, Oct. 2018.
- [19] H. Huang *et al.*, "Deep learning for physical-layer 5G wireless techniques: Opportunities, challenges and solutions," *IEEE Wireless Commun.*, vol. 27, no. 1, pp. 214–222, Feb. 2020.
- [20] Z. Xuan and K. Narayanan, "Analog joint source-channel coding for Gaussian sources over AWGN channels with deep learning," in *Proc. Int. Conf. Signal Process. Commun. (SPCOM)*, Jul. 2020, pp. 1–5.
- [21] T. Wang, C.-K. Wen, S. Jin, and G. Y. Li, "Deep learning-based CSI feedback approach for time-varying massive MIMO channels," *IEEE Wireless Commun. Lett.*, vol. 8, no. 2, pp. 416–419, Apr. 2019.
- [22] M. S. Sim, Y.-G. Lim, S. H. Park, L. Dai, and C.-B. Chae, "Deep learning-based mmWave beam selection for 5G NR/6G with sub-6 GHz channel information: Algorithms and prototype validation," *IEEE Access*, vol. 8, pp. 51634–51646, 2020.
- [23] A. Alkhateeb, S. Alex, P. Varkey, Y. Li, Q. Qu, and D. Tujkovic, "Deep learning coordinated beamforming for highly-mobile millimeter wave systems," *IEEE Access*, vol. 6, pp. 37328–37348, 2018.
- [24] Y. Wang, M. Liu, J. Yang, and G. Gui, "Data-driven deep learning for automatic modulation recognition in cognitive radios," *IEEE Trans. Veh. Technol.*, vol. 68, no. 4, pp. 4074–4077, Apr. 2019.
- [25] M. Mehrabi, M. Mohammadkarimi, M. Ardakani, and Y. Jing, "Decision directed channel estimation based on deep neural network k -step predictor for MIMO communications in 5G," *IEEE J. Sel. Areas Commun.*, vol. 37, no. 11, pp. 2443–2456, Aug. 2019.
- [26] X. Wang, H. Hua, and Y. Xu, "Pilot-assisted channel estimation and signal detection in uplink multi-user MIMO systems with deep learning," *IEEE Access*, vol. 8, pp. 44936–44946, 2020.
- [27] Q. Bai, J. Wang, Y. Zhang, and J. Song, "Deep learning-based channel estimation algorithm over time selective fading channels," *IEEE Trans. Cognit. Commun. Netw.*, vol. 6, no. 1, pp. 125–134, Mar. 2020.
- [28] C. Dong, C. C. Loy, K. He, and X. Tang, "Image super-resolution using deep convolutional networks," *IEEE Trans. Pattern Anal. Mach. Intell.*, vol. 38, no. 2, pp. 295–307, Feb. 2016.
- [29] K. Zhang, W. Zuo, Y. Chen, D. Meng, and L. Zhang, "Beyond a Gaussian denoiser: Residual learning of deep CNN for image denoising," *IEEE Trans. Image Process.*, vol. 26, no. 7, pp. 3142–3155, Jul. 2017.
- [30] J. Li and P. Stoica, "MIMO radar diversity means superiority," in *MIMO Radar Signal Processing*. Hoboken, NJ, USA: Wiley, 2009.
- [31] Y. Zhang, G. Zhang, and X. Wang, "Computationally efficient DOA estimation for monostatic MIMO radar based on covariance matrix reconstruction," *Electron. Lett.*, vol. 53, no. 2, pp. 111–113, Jan. 2017.
- [32] I. Bekkerman and J. Tabrikian, "Target detection and localization using MIMO radars and sonars," *IEEE Trans. Signal Process.*, vol. 54, no. 10, pp. 3873–3883, Oct. 2006.
- [33] X. Zhang, L. Xu, L. Xu, and D. Xu, "Direction of departure (DOD) and direction of arrival (DOA) estimation in MIMO radar with reduced-dimension MUSIC," *IEEE Commun. Lett.*, vol. 14, no. 12, pp. 1161–1163, Dec. 2010.
- [34] L. Li, T. Fu, Y. Yang, M. Huang, Z. Han, and J. Li, "Joint angle estimation and array calibration using eigenspace in monostatic MIMO radar," *IEEE Access*, vol. 8, pp. 60645–60652, 2020.
- [35] F. Wen, D. Huang, K. Wang, and L. Zhang, "DOA estimation for monostatic MIMO radar using enhanced sparse Bayesian learning," *J. Eng.*, vol. 2018, no. 5, pp. 268–273, May 2018.
- [36] A. M. Elbir, "Direction finding in the presence of direction-dependent mutual coupling," *IEEE Antennas Wireless Propag. Lett.*, vol. 16, pp. 1541–1544, 2017.
- [37] A. Liu, G. Liao, C. Zeng, Z. Yang, and Q. Xu, "An eigenstructure method for estimating DOA and sensor gain-phase errors," *IEEE Trans. Signal Process.*, vol. 59, no. 12, pp. 5944–5956, Dec. 2011.
- [38] Y. Rockah and P. Schultheiss, "Array shape calibration using sources in unknown locations—Part I: Far-field sources," *IEEE Trans. Acoust., Speech, Signal Process.*, vol. ASSP-35, no. 3, pp. 286–299, Mar. 1987.
- [39] P. Stoica and A. Nehorai, "Performance study of conditional and unconditional direction-of-arrival estimation," *IEEE Trans. Acoust., Speech, Signal Process.*, vol. 38, no. 10, pp. 1783–1795, Oct. 1990.
- [40] C. Zhang, H. Huang, and B. Liao, "Direction finding in MIMO radar with unknown mutual coupling," *IEEE Access*, vol. 5, pp. 4439–4447, 2017.
- [41] Z.-M. Liu and Y.-Y. Zhou, "A unified framework and sparse Bayesian perspective for direction-of-arrival estimation in the presence of array imperfections," *IEEE Trans. Signal Process.*, vol. 61, no. 15, pp. 3786–3798, Aug. 2013.

- [42] B. Liao, S.-C. Chan, and K.-M. Tsui, "Recursive steering vector estimation and adaptive beamforming under uncertainties," *IEEE Trans. Aerosp. Electron. Syst.*, vol. 49, no. 1, pp. 489–501, Jan. 2013.
- [43] B. Liao and S. C. Chan, "Direction finding with partly calibrated uniform linear arrays," *IEEE Trans. Antennas Propag.*, vol. 60, no. 2, pp. 922–929, Feb. 2012.
- [44] C. Deli, Z. Gong, T. Huamin, and L. Huanzhang, "Approach for wideband direction-of-arrival estimation in the presence of array model errors," *J. Syst. Eng. Electron.*, vol. 20, no. 1, pp. 69–75, 2009.
- [45] N. Gonzalez-Prelcic, R. Mendez-Rial, and R. W. Heath, Jr., "Radar aided beam alignment in mmwave V2I communications supporting antenna diversity," in *Proc. Inf. Theory Appl.*, Feb. 2016, pp. 1–7.
- [46] T. S. Rappaport, E. Ben-Dor, J. N. Murdock, and Y. Qiao, "38 GHz and 60 GHz angle-dependent propagation for cellular peer-to-peer wireless communications," in *Proc. IEEE Int. Conf. Commun. (ICC)*, Jun. 2012, pp. 4568–4573.
- [47] J.-C. Lin, "Least-squares channel estimation for mobile OFDM communication on time-varying frequency-selective fading channels," *IEEE Trans. Veh. Technol.*, vol. 57, no. 6, pp. 3538–3550, Nov. 2008.
- [48] A. Ferreol, P. Larzabal, and M. Viberg, "On the asymptotic performance analysis of subspace DOA estimation in the presence of modeling errors: Case of MUSIC," *IEEE Trans. Signal Process.*, vol. 54, no. 3, pp. 907–920, Mar. 2006.
- [49] Q. S. Ren and A. J. Willis, "Extending MUSIC to single snapshot and on line direction finding applications," in *Proc. Inst. Elect. Eng. Conf. Radar*, no. 449, Oct. 1997, pp. 783–787.
- [50] L. Dai, J. Wang, Z. Wang, P. Tsiaflakis, and M. Moonen, "Spectrum- and energy-efficient OFDM based on simultaneous multi-channel reconstruction," *IEEE Trans. Signal Process.*, vol. 61, no. 23, pp. 6047–6059, Dec. 2013.
- [51] M. Soltani, V. Pourahmadi, A. Mirzaei, and H. Sheikhzadeh, "Deep learning-based channel estimation," *IEEE Commun. Lett.*, vol. 23, no. 4, pp. 652–655, Apr. 2019.



Sai Huang (Member, IEEE) is currently working with the Department of Information and Communication Engineering, Beijing University of Posts and Telecommunications, and also serves as the Academic Secretary for the Key Laboratory of Universal Wireless Communications, Ministry of Education, China. He is a reviewer of international journals, such as *IEEE TRANSACTIONS ON WIRELESS COMMUNICATIONS*, *IEEE TRANSACTIONS ON VEHICULAR TECHNOLOGY*, *IEEE WIRELESS COMMUNICATIONS LETTERS*, and *IEEE TRANSACTIONS ON COGNITIVE COMMUNICATIONS AND NETWORKING*, and international conferences, such as IEEE ICC and IEEE GLOBECOM. His research interests include machine learning assisted intelligent signal processing, statistical spectrum sensing and analysis, fast detection and depth recognition of universal wireless signals, millimeter wave signal processing, and cognitive radio networks.



Meng Zhang (Graduate Student Member, IEEE) is currently pursuing the M.S. degree with the Beijing University of Posts and Telecommunications. Her research interests include channel estimation and millimeter wave communications.



Yicheng Gao (Student Member, IEEE) received the B.Sc. degree in communication engineering from the University of Science and Technology Beijing in 2017 and the M.Sc. degree in information and communication engineering from the Beijing University of Posts and Telecommunications in 2020. She is currently pursuing the Ph.D. degree in computing with Imperial College London. Her research interests include 5G, the IoT, FaaS, channel estimation and tracking, edge computing, resource provisioning, and QoS/SLA management.



Zhiyong Feng (Senior Member, IEEE) received the B.S., M.S., and Ph.D. degrees in information and communication engineering from the Beijing University of Posts and Telecommunications (BUPT), Beijing, China. She is currently a Full Professor. She is also the Director of the Key Laboratory of Universal Wireless Communications, Ministry of Education. Her research interests include wireless network architecture design and radio resource management in 5th generation mobile networks (5G), spectrum sensing and dynamic spectrum management in cognitive wireless networks, universal signal detection and identification, and network information theory. She is also a Technical Advisor of NGMN, an Editor of *IET Communications* and *KSI Transactions on Internet and Information Systems*, and a Reviewer of *IEEE TRANSACTIONS ON WIRELESS COMMUNICATIONS* (TWC), *IEEE TRANSACTIONS ON VEHICULAR TECHNOLOGY* (TVT), and *IEEE JOURNAL ON SELECTED AREAS IN COMMUNICATIONS* (JSAC). She is active in ITU-R, IEEE, ETSI, and CCSA standards.